Ammonia borane oxidation at gold microelectrodes in alkaline solutions.

Lorraine C. Nagle and James F. Rohan*

Tyndall National Institute, University College Cork, Lee Maltings, Cork, Ireland.

* Corresponding author. Tel.: +353 21 4904224; Fax: +353 21 4270271.

***E-mail address*: james.rohan@tyndall.ie (James F. Rohan).**

Abstract

Borane based electroless plating baths are of interest in many microelectronics applications such as barrier/capping layers for copper IC interconnect. To optimise the plating baths a thorough understanding of the role of the bath constituents is required. To this end we have employed microelectrodes to investigate the oxidation mechanism of boranes in alkaline solutions. In this paper we present data for the simpler ammonia borane (AB) oxidation and compare it with the previous analysis of dimethyl amine borane (DMAB) oxidation. Both AB and DMAB are shown to oxidise in two steady state mass transport controlled oxidation waves for specific concentration ranges. Particular emphasis is placed on the analysis of the second oxidation wave observed at less negative potentials and the differences observed in the analysis of AB and DMAB in this potential region. The potential range for oxidation, the optimum concentration and a suggested mechanism for oxidation are shown.

1. Introduction.

The oxidation of amine boranes in aqueous solutions is increasingly being investigated to optimise the low cost deposition of materials such as metals [1-8], semiconductors [9,10] and insulators [11] through electroless processing for microtechnology applications. Boranes and borohydrides have an advantage over the most widely used alternative reducing agent, hypophosphite, of being catalytically oxidised at technologically significant substrates such as copper without the requirement for substrate palladium activation [12] which reduces the number of processing steps and can aid selectivity. Furthermore, the boron content in deposits is significantly lower than the phosphorus codeposit from hypophosphite based baths leading to purer deposits of the desired material. Boranes and borohydrides are also a nontoxic alternative to formaldehyde and hydrazine. There has also been an increased activity in the analysis of boranes [13,14] or borohydride materials as fuels for fuel cell systems [15-19]. In the optimisation of plating baths or catalysts for the fuel cell systems it is desirable to know the likely oxidation mechanism for the reducing agent or fuel material. The multielectron reactions that occur during the complete oxidation of boranes or borohydrides have complicated attempts to decipher the oxidation mechanism. A recent review of electroless deposition concluded that further analysis is required to study the reducing agent reactions [20]. This study is intended to provide additional parameter information through microelectrode analysis of the borane oxidation reactions with relevance to electroless deposition and fuel cell reactions with particular reference to the simpler AB by comparison with DMAB.

Microelectrodes have inherent qualities that facilitate the acquisition of high quality data [21]. In the specific case of borane oxidation, simple, dilute solutions may be investigated and they have been shown to yield data undistorted by ohmic drop or complications introduced by added electrolyte. Previous analysis in this laboratory [22] of the DMAB oxidation reaction at a gold microdisk in 1 mol dm^{-3} NaOH led to the determination of the diffusion coefficient and apparent coulomb number. The oxidation mechanism proposed therein made allowance for the possible complication of hydrogen gas evolution at lower ratios of hydroxide ion to borane. The microelectrode data indicated that for DMAB the oxidation proceeds via an irreversible three-electron oxidation followed by a second irreversible wave at more positive potentials of equal height and presumably equal electron transfer. The second wave was shown to be complicated by gold monolayer oxide and a true plateau was difficult to achieve. The first wave which occurs 500 mV more negative than the second wave has been attributed to the oxidation of an intermediate BH_3OH^- that does not appear to occur during the borohydride oxidation process in 1 mol dm^{-3} NaOH [23]. This apparent three-electron oxidation [22] is therefore in a more favourable potential region for electroless deposition given that the area of overlap of the oxidation and reduction reactions is significantly larger than for borohydride systems and would potentially lead to a cell voltage increase for fuel cells based on this system. We describe here the analysis of a simpler AB complex to probe the two wave oxidation of the boranes and compare the oxidation behaviour with that of DMAB. The AB is itself a potential reducing agent/fuel for specific applications and the parameters determined in this work are necessary to assist in the characterisation of any system in which it is employed.

2. Experimental.

The borane complexes utilised in this work DMAB and AB (minimum purity 97 %) and sodium hydroxide (NaOH) (minimum purity 99 %) were purchased from Sigma Aldrich and used as received. Deionised water of resistivity 18 MΩ cm was used to prepare all solutions. The working electrode was a 10 μm diameter Au microdisk (Princeton Applied Research) supplied by Advanced Measurement Technology, UK. This was polished with 0.5 μm alumina powder obtained from Struers on a Buehler polishing cloth for 1-2 minutes and rinsed in deionised water. A 0.5 mm diameter Pt counter electrode of 37 mm length was supplied by IJ Cambria. Cyclic voltammograms (CV) or linear sweep voltammograms (LSV) were recorded with respect to a Ag/AgCl, KCl saturated reference electrode (also supplied by IJ Cambria). The potential of the working electrode was controlled using a CH Instruments potentiostat model 620A with picoamp booster. The effective cell volume was 20 ml. All solutions were purged with nitrogen for 20 minutes prior to experiments in order to remove oxygen and the experiments were performed at 20 ^{o}C.

3. Results and Discussion.

Au microelectrodes in strongly alkaline solutions have been used to investigate the AB oxidation reaction. This system permits analysis of dilute solutions without additional supporting electrolyte. In addition a negligible background current at Au in the potential region corresponding to AB oxidation also assists in this analysis. In strongly alkaline solution it is expected that AB, like DMAB [3,24-27], will exist as

the hydroxytrihydroborate ion, $BH_3(OH)^-$, which may undergo oxidation with maximum coulombic efficiency on Au in base according to the reaction,

$$BH_3(OH)^- + 6OH^- = B(OH)_4^- + 3H_2O + 6e^- \quad [1]$$

Competing chemical hydrolysis of AB with evolution of hydrogen, given by equation 2, is expected to be minimal in this solution [27]. Previous analysis [22] has indicated a concentration range over which full coulombic efficiency may be observed and at what level of hydroxide ion to borane in solution the hydrogen evolution reaction [Eqn 2] is expected to become significant. Lower coulombic efficienvy may be expected in less alkaline solutions.

$$BH_3(OH)^- + 3\ H_2O = B(OH)_4^- + 3H_2 \quad [2]$$

Typical behaviour for gold in 1 mol dm^{-3} NaOH is seen in the CV recorded over the potential range -1.15 to +0.68 V for a 10 μm diameter microdisk electrode shown in Fig 1. This voltammogram shows that negligible current (subnanoamp) flows in the absence of AB over the potential range -1.15 to +0.05 V. The onset of monolayer oxide formation is shown to occur above +0.05 V with the corresponding oxide reduction peak on the reverse sweep.

When 20 mmol dm^{-3} AB is added to the 1 mol dm^{-3} NaOH solution a well-defined CV (Fig. 2(a)) is achieved at a Au microdisk consisting of two irreversible anodic waves. Mass transport-controlled steady-state currents were recorded for the first and second waves at –0.65 V and -0.15 V, respectively. The voltammograms exhibit a

pronounced plateau region upon sweeping the potentials to more positive values unlike that observed for DMAB in the case of the second wave. The current then decreases as the potential is swept into the gold monolayer oxide region as reported previously for DMAB [7,22,26]. The magnitude of the current for both anodic waves is equal and increases linearly with concentration of AB up to 40 mmol dm^{-3}, Figs 2(b) and 2(c). The fit to the data shown in Fig 2(c) indicates that unlike that observed for DMAB on the forward sweep the AB oxidation current increase in the second wave is linear with concentration added and not complicated by gold oxide behaviour at the electrode. When the AB concentration exceeded 50 mmol dm^{-3} the measured currents did not increase linearly with AB concentration and the reverse sweep did not retrace the forward sweep. In these cases the evolution of gas, presumably hydrogen, was obvious.

The AB solution is a simpler system than DMAB with current overlap of the oxidation current on the forward and reverse sweeps at potentials more negative than 0.05V. By comparison, DMAB exhibits complications in the second wave [22] with the forward sweep giving a lower oxidation current than the reverse sweep. The removal of monolayer oxide leads to the increased current observed, however, the mass transport controlled DMAB oxidation only achieves the same magnitude as the first wave on the reverse sweep. The reverse sweeps of CV's are shown in Fig 3(a) for a series of concentrations of DMAB. The steady state currents achieved for both waves are plotted in Fig 3(b). The linear nature of the current increase with increasing concentration on the reverse sweep is indicative of a mass transport controlled reaction for both waves. The data in Fig. 3(b) shows that the current achieved for the

first wave is slightly higher than the second wave even when the data is taken from the reverse sweep.

It appears that the oxidation of DMAB is impeded by other species in addition to the complication caused by formation of gold monolayer oxide. In the oxidation wave of DMAB the forward and reverse currents start to diverge at potentials more positive than -0.25V. AB oxidation is not impeded in this way even on the forward sweep until approx -0.06V after which it is assumed the same surface oxide should be present in the otherwise identical electrolyte. Dimethylamine was added to the solution to examine its possible influence on the reaction. The results are shown in Fig. 4. The gradual addition of dimethylamine to a 10 mmol dm^{-3} solution AB in 1 mol dm^{-3} NaOH results in a decrease in magnitude of the current for the second anodic wave and at very high concentrations the first wave is also influenced to an extent. The second oxidation wave for AB becomes drawn out and the plateau current becomes less obvious before the potential reaches the gold monolayer oxide region. This behaviour is observed on forward scans for solutions of DMAB. It is suggested that the dimethylamine has an influence on the borane oxidation reaction by non-Faradaic surface interactions at the electrode leading to a decrease in the magnitude of the second oxidation wave. It has been assumed that the amine boranes are in the dissociated state in these solutions which leads to the conclusion that it is the dimethylamine adsorbing on the substrate that leads to the current decrease rather than interaction in the solution removed from the substrate.

The oxidation of AB was further analysed to determine the diffusion coefficient in this medium using a technique introduced by Bard et al [27]. Microelectrodes enable

the determination of the diffusion coefficient without a prior knowledge of n. The coulomb number has not been previously demonstrated and hence this analysis is required to extract the unknown parameters. As stated earlier, the diffusing species in this 1 mol dm^{-3} NaOH solution is likely to be BH_3OH^-. The diffusion coefficient was determined directly by analysing the chronoamperometric response for the first anodic wave which reaches a steady state at -0.65 V. The current transient in response to a potential step from –1.15 to –0.65 V was recorded for 20 mmol dm^{-3} AB in 1 mol dm^{-3} NaOH. The D value determined is 8.45×10^{-6} cm^2 s^{-1}. This is similar to the value determined for DMAB (7.48×10^{-6} cm^2 s^{-1}) in an identical electrolyte [22]. It remains considerably lower than the value estimated by Bard et al [27] (1.68×10^{-5} cm^2 s^{-1}) for the BH_4^- species in the borohydride analysis

Using the expression for the limiting current, I, under mass transport-controlled, steady state conditions at a microdisk electrode (equation 5) and 8.45×10^{-6} cm^2 s^{-1} for D, the coulomb number, n, was found to be 3.3.

$$I = 4nFDrC \qquad [5]$$

where r is microdisk radius and C is concentration of AB.

It is assumed here that the diffusion coefficient for both oxidation waves represented in Fig 2(a) is the same. Hence, given that the oxidation current associated with the first and second stages is equal, a value of three for n has also been assigned to the second oxidation stage, implying a total six-electron loss for AB oxidation. It has been observed earlier in solutions where BH_4^- hydrolysis had occurred [24,25,28] that

oxidation waves separated by 500 mV could be attributed to BH_3OH^- and BH_4^- oxidation. This separation is shown in Fig.5 for solutions of AB, DMAB and $NaBH_4$. The currents achieved for BH_4^- oxidation are higher for smaller concentrations. This is most likely a result of the faster diffusion of the BH_4^- [23,27] by comparison with BH_3OH^- [22].

Ab initio molecular orbital order modelling of the DMAB reaction pathway has been investigated [6,29] where the reaction intermediate was considered to be 3 or 5 coordinate. From this work it appears that during the oxidation process the reaction pathway exhibits a potential shift following the third electron transfer which indicates that the intermediate at this point is more stable than the others in the mechanism. The suggested reaction pathway for AB and DMAB oxidation may be represented by equations 6 to 9 depending on whether 5 coordinate or 3 coordinate species, respectively, are more stable at the midpoint of the borane oxidation. The techniques employed in this study cannot reveal the identity of these species or whether they are 5 or 3 coordinate. Further analysis of these systems such as those proposed in [20] is required to identify the intermediates involved for this technologically relevant system.

Reaction pathway:

$$BH_3(OH)^- + 3OH^- = BH_2(OH)_3^- + 3e^- + H_2O \quad [6]$$

$$BH_2(OH)_3^- + 3OH^- = B(OH)_4^- + 3e^- + 2H_2O \quad [7]$$

or

$$BH_3(OH)^- + 3OH^- = BH(OH)_2^- + 3e^- + 2H_2O \quad [8]$$

$$BH(OH)_2^- + 3OH^- = B(OH)_4^- + 3e^- + H_2O \quad [9]$$

4. Conclusion

Microelectrodes have been utilised to acquire data for the oxidation of AB which has been compared with results achieved for DMAB and borohydride. As in the case of DMAB two oxidation waves have been observed for AB. Data was acquired at microelectrodes to independently determine the diffusion coefficient for the AB. Using the D value determined the coulomb number assigned to both of the oxidation waves was three. The six-electron oxidation reaction is dependent on the concentration of AB in 1 M NaOH. At concentrations greater than 50 mmol dm^{-3} AB oxidation also evolves hydrogen gas and the coulomb number is less than six. It is suggested that the species being oxidised in the second wave for borane is similar to that of the latter stages of borohydride oxidation as exemplified by the overlapping potential range for this reaction. AB and borohydride exhibit simpler voltammograms than DMAB. The introduction of dimethylamine independently appears to complicate the reaction process for AB at the surface of the electrode particularly for the second oxidation wave.

Acknowledgements.

The authors thank the Irish Research Council for Science, Engineering and Technology (IRCSET) for financial support.

References.

1. F. Pearlstein and R.F.Weightman, *Plat.*, **60**, 474 (1973)
2. M. Lelental, *J. Catal.*, **32**, 429 (1974).
3. C.D. Iacovangelo, *J. Electrochem. Soc.,* **138**, 976 (1991).
4. J.C. Patterson, C. Ni Dheasuna, J. Barrett, T.R. Spalding, M. O'Reilly, X.Jiang and G.M. Crean, *Appl. Surf. Sci.,* **91**, 124 (1995)
5. A. Chiba, H. Haijima and K. Kobayashi*, Surf. Coat. Tech.,* **169-170**, 104 (2003).
6. T. Homma, A. Tamaki, H. Nakai and T. Osaka, *J. Electroanal. Chem.,* **559**.131 (2003).
7. A. Sargent, O. Sadik and L. Matienzo, *J. Electrochem. Soc.,* **148,** C257 (2001).
8. Y. Yamauchi, T. Yokoshima, H. Mukaibo, M. Tezuka, T. Shigeno, T. Momma, T. Osaka and K. Kuroda, *Chem. Lett.,* **33**, 542 (2004).
9. J.M. Izaki and T. Omi, *J. Electrochem.Soc.,* **144**, L3 (1997).
10. M. Izaki and J.Katayama, *J. Electrochem. Soc.,* **147,** 210 (2000).
11. M. Chigane, M. Izaki, T. Shinagawa and M. Ishikawa, *Electrochem. Solid-State Lett.,* **7**, D1 (2004).
12. T. Osaka, N.Takano, T.Kurokawa, T.Kaneko and K.Ueno. *Surf. Coat. Tech.,* **169–170,** 124 (2003)
13. A. Gutowska, L. Li, Y. Shin, C.M. Wang, X.S. Li, J.C. Linehan, R.S. Smith, B.D. Kay, B. Schmid, W. Shaw, M. Gutowski and T. Autrey, *Angew. Chem. Int. Ed.,* **44**, 3578, (2005)
14. Y. Chen, J.L. Fulton, J.C. Linehan and T. Autrey, *J. Am. Chem. Soc.;* **127**, 3254 (2005)

15. E. Gyenge, *Electrochim. Acta,* **49** 965 (2004)

16. Z.P. Li., B.H. Liu, K. Arai, K. Asaba, S. Suda, *J. Power Sources,* **126**, 28 (2004)

17. B.H. Liu, Z.P. Li and S. Suda, *J. Electrochem. Soc.,* **150**, A398 (2003)

18. A. Verma and S. Basu. *J.Power Sources,* **145,** 282 (2005)

19. B.H. Liu, Z.P. Li, K. Arai, S. Suda, *Electrochim. Acta,* **50,** 3719 (2005)

20. E.J. O'Sullivan, *Advances in electrochemical science and engineering,* Volume 7, R.C.Alkire and D.M.Kolb Editors, p. 225 Wiley, New York, (2001)

21. D. Pletcher, *Microelectrodes: Theory and Application,* M. I. Montenegro, M. A. Queirós and J. L. Daschbach, Editors, p. 3, Kluwer Academic Publishers, Dordrecht, (1991)

22. L.C. Nagle and J.F. Rohan, *Electrochem. Solid-State Lett.,* **8**, C77 (2005)

23. M.V. Mirkin, H. Yang and A.J. Bard, *J. Electrochem. Soc.,* **139**, 2212 (1992).

24. J.A. Gardiner and J.W. Collat, *J. Am. Chem. Soc.,* **87**, 1692 (1965).

25. J.A. Gardiner and J.W. Collat, *Inorg. Chem.,* **4**, 1208 (1965).

26. L.D. Burke and B.H. Lee, *J. Appl. Electrochem.,* **22**, 48 (1992)

27. G. Denault, M. Mirkin and A.J. Bard, *J. Electroanal. Chem.,* **308**, 27 (1991).

28. Y. Okinaka, *J. Electrochem. Soc.,* **120,** 739 (1973).

29. T. Homma, H. Nakai, M. Onishi and T. Osaka, *J.Phys. Chem. B,* **103,** 1774 (1999).

Figure legends.

Figure 1 CV (-1.15 to +0.68 V) at Au microdisk in 1 mol dm^{-3} NaOH at 100 mV s^{-1}.

Figure 2(a). CV (-1.15 to 0.45 V) of 20 mmol dm^{-3} AB at Au microdisk in 1 mol dm^{-3} NaOH at 100 mV s^{-1}.

Figure 2(b). LSV (-1.15 to -0.055 V) of AB (a) 1.1, (b) 7.2, (c) 16.2, (d) 20 and (e) 40 mmol dm^{-3} at gold microdisk in 1 mol dm^{-3} NaOH at 100 mV s^{-1}.

Figure 2(c). Plot of steady-state current at –0.15 V for second oxidation wave vs. concentration for AB at gold microdisk in 1 mol dm^{-3} NaOH at 100 mV s^{-1}

Figure 3(a). CV (-1.15 to 0.45 V) of DMAB (a) 0.9, (b) 8, (c) 17, (d) 36 and (e) 70 mmol dm^{-3} at gold microdisk in 1 mol dm^{-3} NaOH at 100 mV s^{-1}. For clarity the data shown is the reverse sweep from 0.085V to -1.15V only, which exhibits higher current for the second wave at 0.05V.

Figure 3(b) Plot of steady-state currents at ● –0.65 V and ■ 0.0V (current at -0.65 V subtracted) for DMAB at a gold microdisk in 1 mol dm^{-3} NaOH at 100 mV s^{-1}. Data is taken from the reverse sweep of the voltammograms.

Figure 4. CV (-1.15 to -0.02 V) of 10 mmol dm^{-3} AB with (a) 0, (b) 10, (c) 30 (d) 100 and (e) 200 mmol dm^{-3} dimethylamine added at gold microdisk in 1 mol dm^{-3} NaOH at 100 mV s^{-1}.

Figure 5. LSV (-1.15 to 0.45 V) of (1) 10 mmol dm^{-3} AB (2) 10 mmol dm^{-3} DMAB and (3) 8 mmol dm^{-3} $NaBH_4$ at gold microdisk in 1 mol dm^{-3} NaOH at 100 mV s^{-1}.

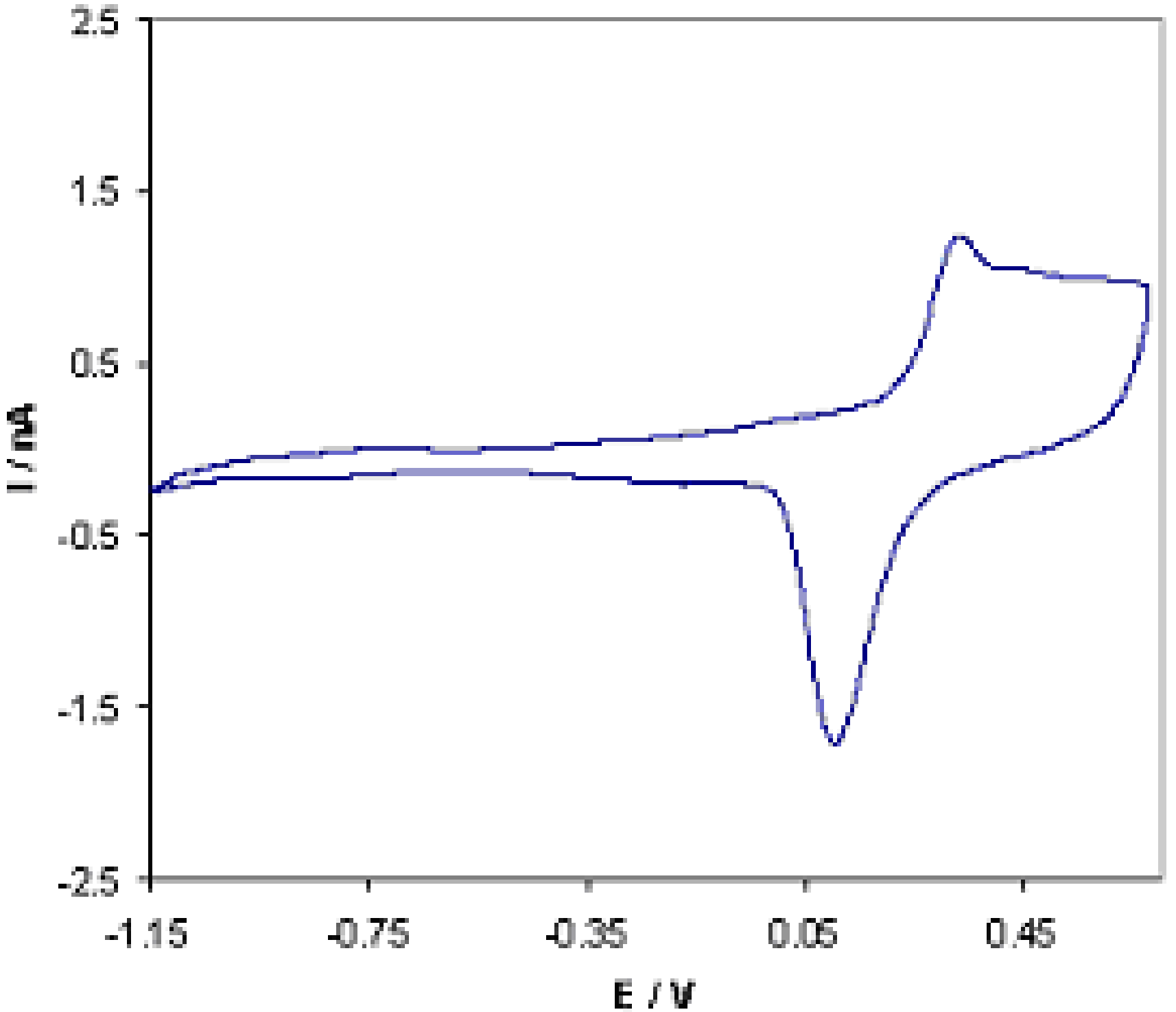
2.5
1.5
0.5
-0.5
-1.5
-2.5
I / mA
-1.15
-0.75
-0.35
0.05
0.45
E / V

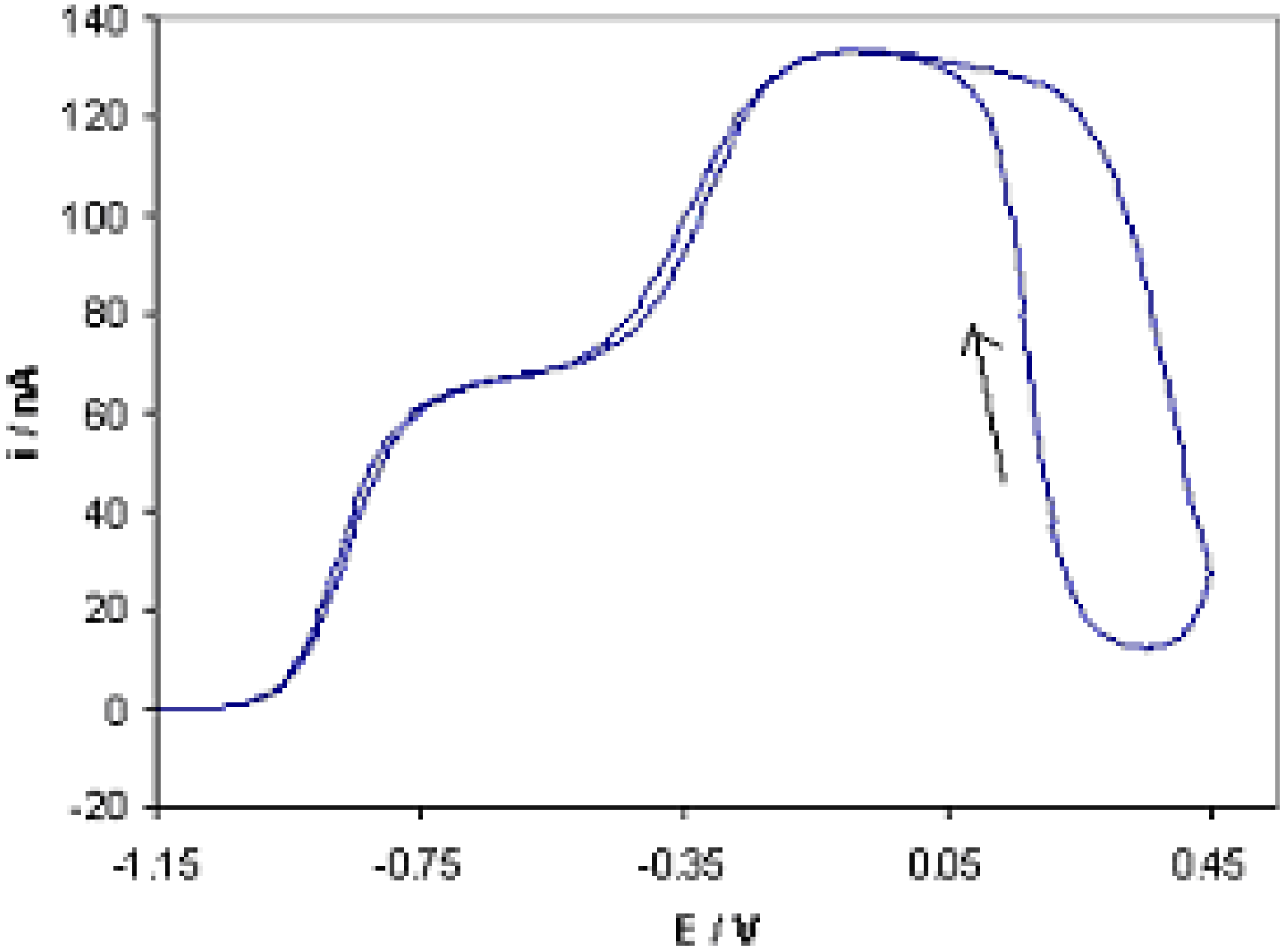
140
120
100
80
60
40
20
0
-20
i / mA
-1.15
-0.75
-0.35
0.05
0.45
E / V

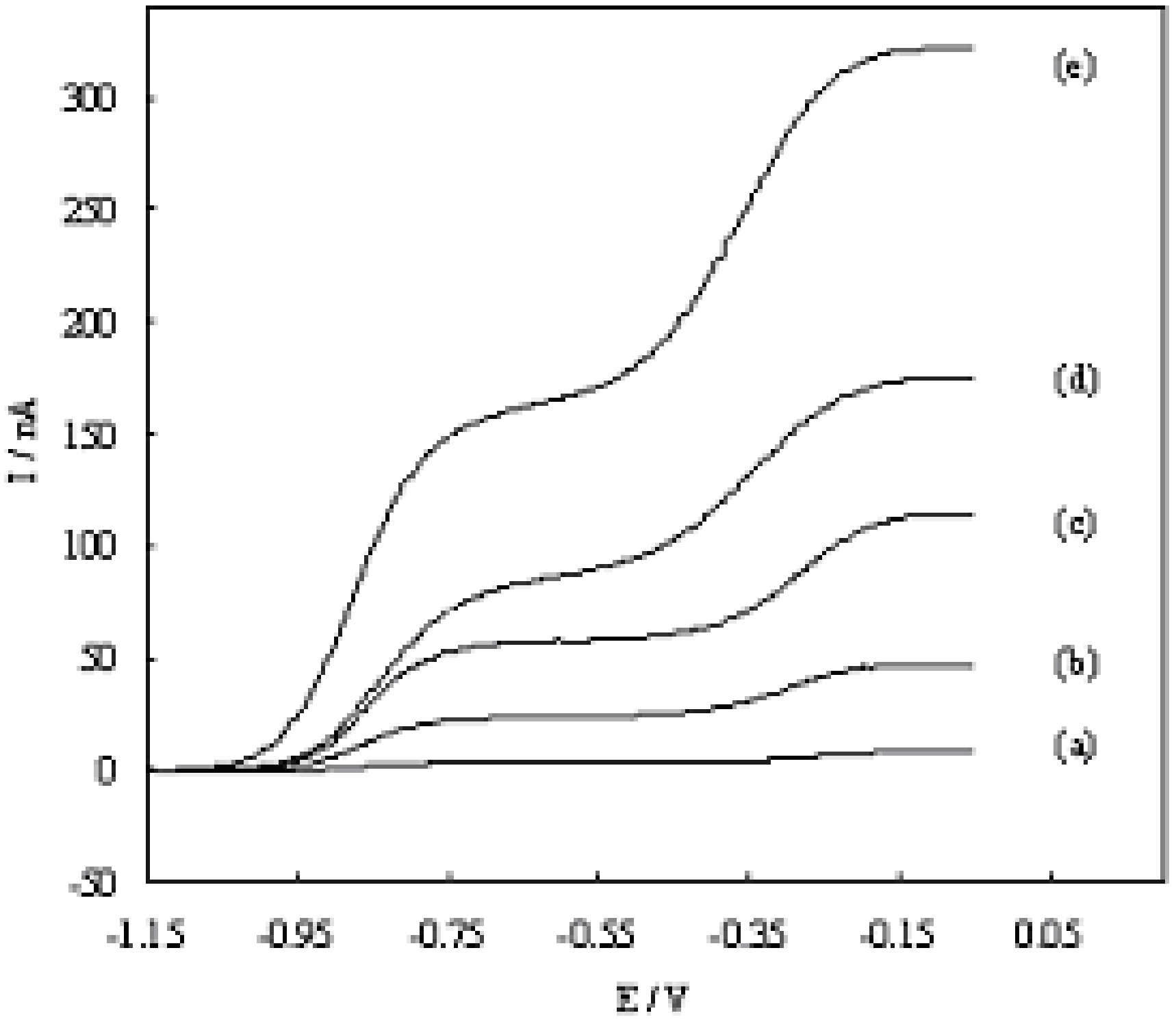
300
250
200
150
100
50
0
-50
I / nA
-1.15
-0.95
-0.75
-0.55
-0.35
-0.15
0.05
E / V
(e)
(d)
(c)
(b)
(a)

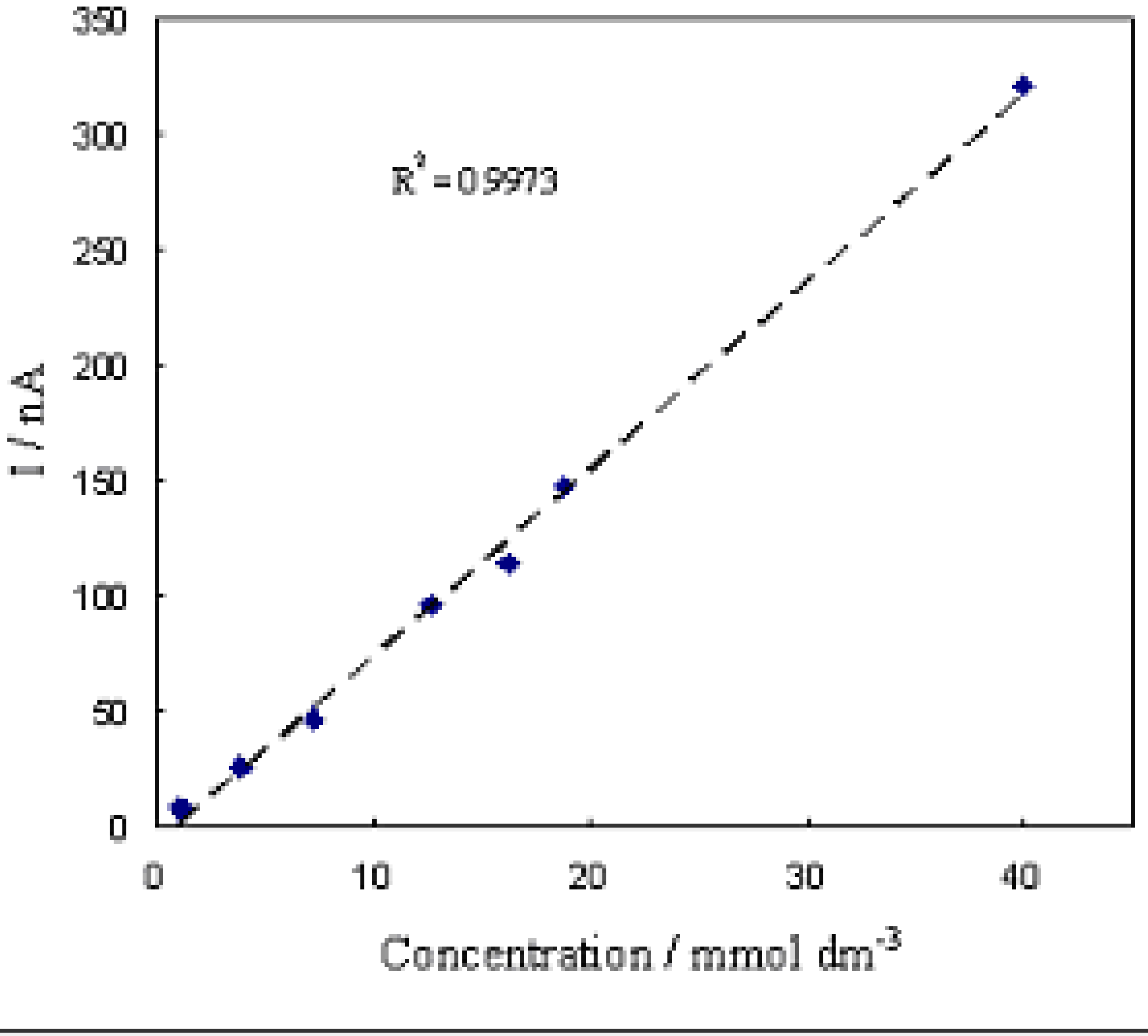
350
300
250
200
150
100
50
0
I / nA
$R^2 = 0.9973$
0
10
20
30
40
Concentration / mmol dm^{-3}

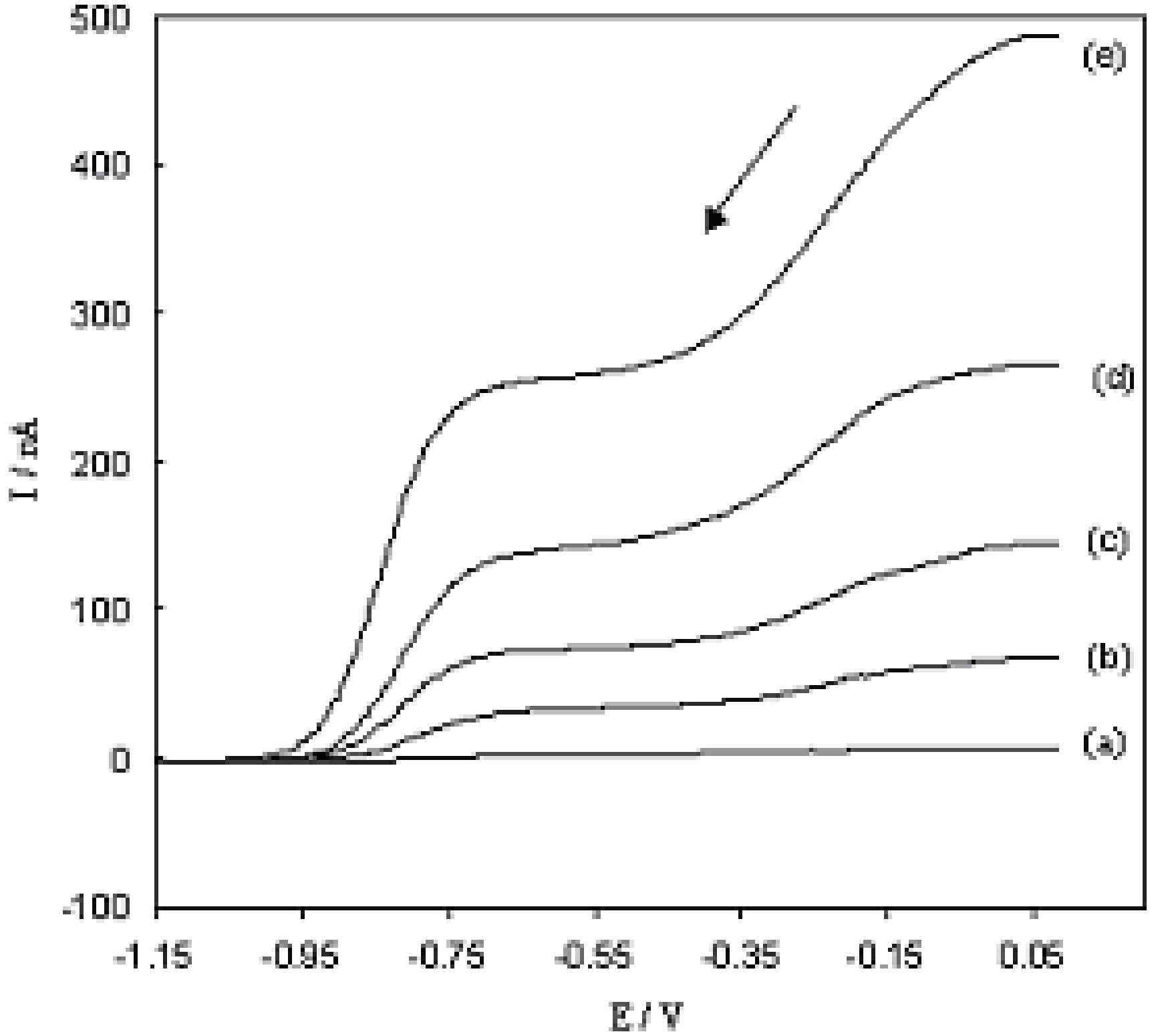
500
400
300
200
100
0
-100
I / nA
-1.15
-0.95
-0.75
-0.55
-0.35
-0.15
0.05
E / V
(e)
(d)
(c)
(b)
(a)

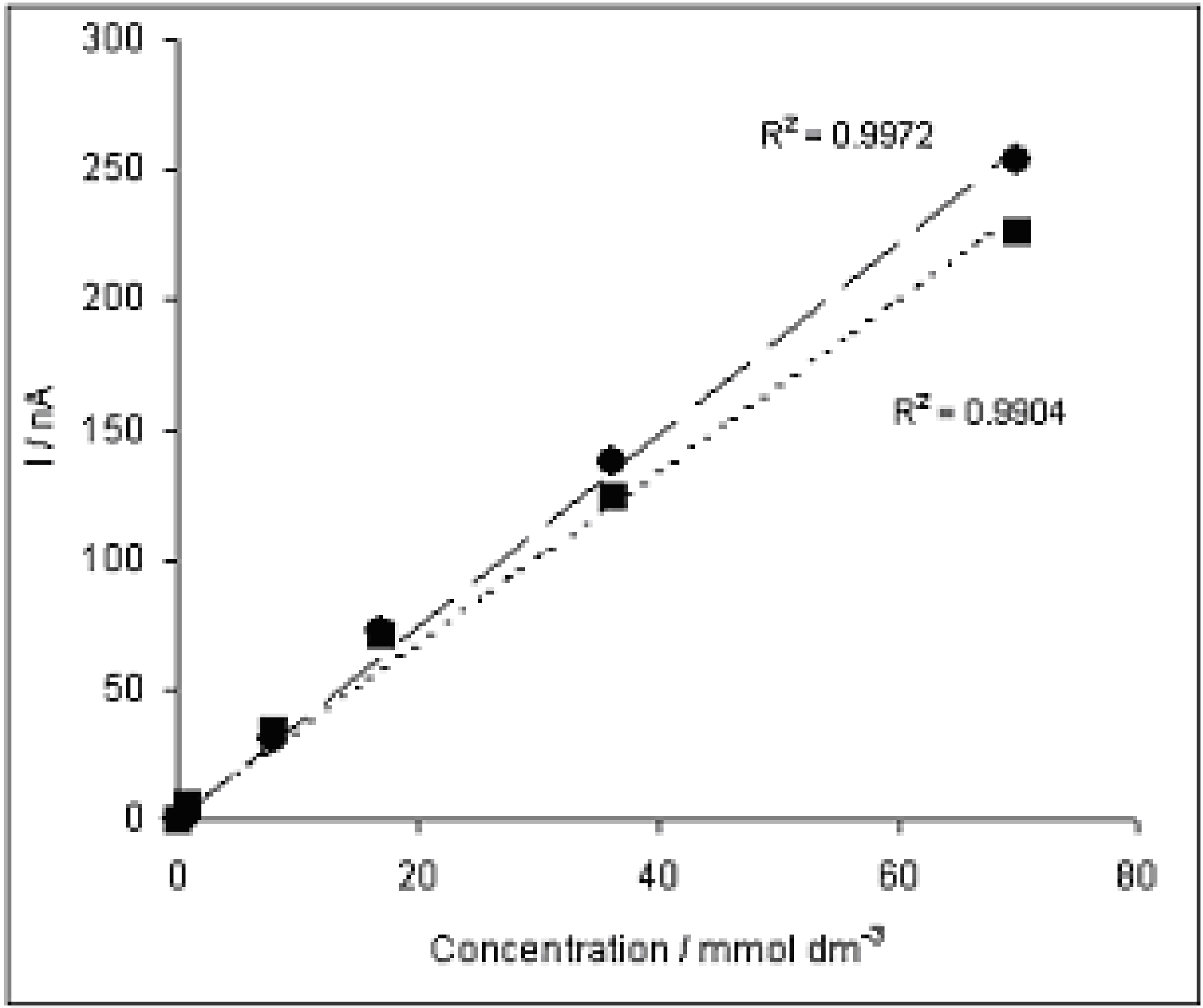
300
250
200
150
100
50
0
I / nA
0
20
40
60
80
Concentration / mmol dm-3
R2 = 0.9972
R2 = 0.9804

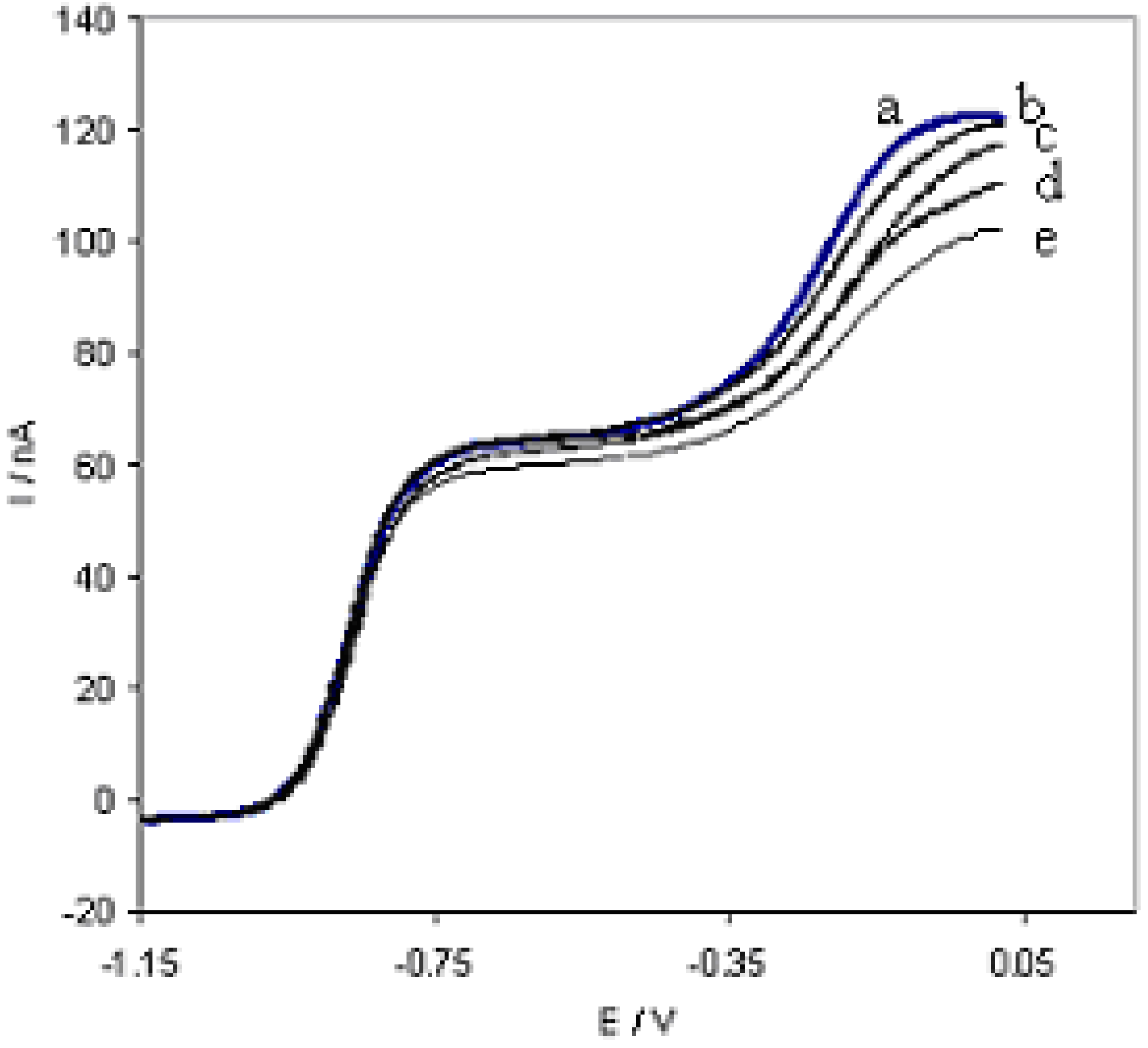
140
120
100
80
60
40
20
0
-20
I / nA
-1.15
-0.75
-0.35
0.05
E / V
a
b
c
d
e

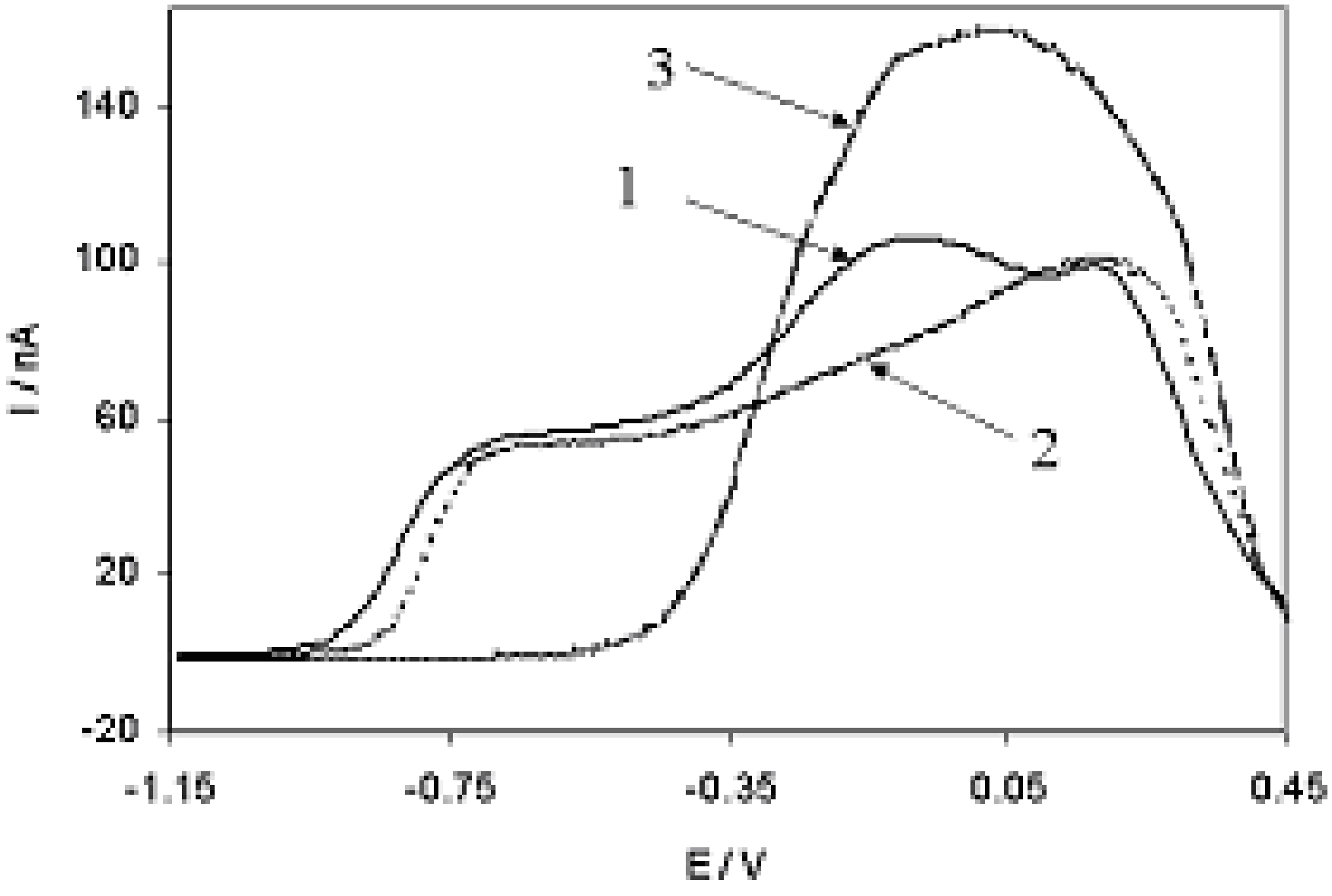
140
100
60
20
-20
I / nA
-1.15
-0.75
-0.35
0.05
0.45
E / V
1
2
3